THE ASTROPHYSICAL JOURNAL, 492:696–702, 1998 January 10

GAMMA-RAY–BURST SPECTRAL SHAPES FROM 2 keV TO 500 MeV

BRADLEY E. SCHAEFER,[1] D. PALMER,[2] B. L. DINGUS,[3] E. J. SCHNEID,[4] V. SCHOENFELDER,[5]
J. RYAN,[6] C. WINKLER,[7] L. HANLON,[8] R. M. KIPPEN,[9] AND A. CONNORS[6]
Received 1997 April 10; accepted 1997 August 14

ABSTRACT

We present three gamma-ray–burst spectra for bright bursts over very wide energy ranges. These were created from BATSE, COMPTEL, and OSSE data. The three spectra are for GRB 910503 (from 20 keV to 300 MeV), GRB 910601 (from 28 keV to 10.5 MeV), and GRB 910814 (from 103 keV to 500 MeV). A composite spectrum of 19 bright bursts is presented from 41 keV to 1.9 MeV (with no weak lines visible) for use in calculating average redshift corrections in cosmological models. Expanding fireball models with shocked synchrotron emission are predicted to have low-energy spectral slope ($\nu F_\nu \propto \nu^\alpha$) that asymptotically approaches $\alpha = 4/3$ such that α should never exceed 4/3. This prediction is tested with more than 100 bright bursts with BATSE and *Ginga* data. Over 90% of the bursts have spectral slopes in agreement with this prediction. For only one burst (GRB 870303, which has reported cyclotron lines) can a strong case be made that the slope violates the model limit, and then only from 2–5 keV.

Subject heading: gamma rays: bursts

1. INTRODUCTION

The spectra of gamma-ray bursts (GRBs) provides the primary input into our understanding of the burst radiation emission mechanisms. Before the launch of the *Gamma Ray Observatory*, the observed energy range was relatively small, so that the continuum shapes appear basically as a power law with some curvature. Such a shape can be explained by many physical models or emission mechanisms.

The *Gamma Ray Observatory* has four instruments (BATSE, EGRET, COMPTEL, and OSSE) that can record burst spectra from roughly 20 keV to 10 GeV. Infrequently, a bright burst will appear within the fields of view of several instruments. The spectra from the individual instruments can then be combined to form one spectrum over a broad energy range. We report on such combined spectra for three bright bursts (§ 2).

To study the average spectral shape, we have averaged spectra from up to 20 bright BATSE bursts into one composite spectrum (§ 3). This composite can be used to search for weak spectral lines or for redshift corrections in cosmological models.

Recent general models of emission mechanisms have predicted that the low-energy spectral slope should asymptotically approach $\nu F_\nu \propto \nu^{4/3}$. In § 4, we use 117 spectra from BATSE and *Ginga* to test this prediction on the shape of the spectrum.

[1] Department of Physics, Yale University, P.O. Box 208121, New Haven, CT 06520-8121.
[2] Universities Space Research Association, Goddard Space Flight Center, Code 661, Greenbelt, MD 20771.
[3] Physics Department, JFB 201, University of Utah, Salt Lake City, UT 84112.
[4] Grumman Aerospace Corporation, R&D Center, MS A01-26, Bethpage, NY 11714.
[5] Max-Planck-Institut für Extraterrestrische Physik, 8046 Garching, Germany.
[6] University of New Hampshire, Space Science Center, Morse Hall, Durham, NH 02384.
[7] Space Sciences Department, European Space Agency, ESTEC, 2200 AG Noordwijk, The Netherlands.
[8] University College Dublin, Stillorgan Road, Belfield, Dublin 4, Ireland.
[9] Center for Space Plasma, University of Alabama, Huntsville, AL 35899.

2. THREE BURST SPECTRA FROM 20 keV TO 500 MeV

We concentrate on three bright bursts which have been detected by three or four *Gamma Ray Observatory* instruments. GRB 910503 and GRB 910814 were seen by BATSE, EGRET, and COMPTEL, while GRB 910601 was seen by all four instruments. Detailed cross comparisons of the spectra for these bursts demonstrated matching fluxes, and this provided early confidence in the calibrations of all four instruments (e.g., Share et al. 1994).

Earlier analyses of these bursts have already been reported for the individual instruments. Spectra for GRB 910503 have been presented for BATSE in Schaefer et al. (1994), for EGRET in Schneid et al. (1992), and for COMPTEL in Winkler et al. (1992). Spectra for GRB 910601 have been presented for BATSE in Schaefer et al. (1994), for EGRET in Kwok et al. (1993), for COMPTEL in Winkler et al. (1993), and for OSSE in Share et al. (1994). Spectra for GRB 910814 have been presented for BATSE in Schaefer et al. (1994), for EGRET in Kwok et al. (1993), and for COMPTEL in Hanlon et al. (1994). The data from individual instruments for each burst are tabulated in Table 1.

For each instrument, the burst spectra were extracted, live-time corrected, background subtracted, and deconvolved with the normal analysis routines. Spectral analysis procedures are reported in Schaefer et al. (1994), Schneid et al. (1992), Hanlon et al. (1994), and Share et al. (1992). The resulting photon spectra have units of photons s^{-1} cm^{-2} keV^{-1}.

The spectra were individually deconvolved for each instrument with either a power law or a sharply broken power-law spectral model. Deconvolved spectra depend to some extent on the assumed model. Fortunately, there are many conditions for which this model dependence will be insignificant. For example, the EGRET spectra are all consistent with a power law and the lower energy curvature is irrelevant since the low-energy photons cannot appear as high-energy photons. The BATSE deconvolution has been found to be very robust, even when a bad spectral shape was assumed (see Figs. 11, 24, 52, and 53 of Schaefer et al. 1994). For each burst, the same spectral models were assumed for the various detectors, and the resulting spectra are consistent from instrument to instrument.

TABLE 1

ENERGY RANGES FOR INPUT SPECTRA

INSTRUMENT	GRB 910503		GRB 910601		GRB 910814	
	E_{low} (keV)	E_{high} (MeV)	E_{low} (keV)	E_{high} (MeV)	E_{low} (keV)	E_{high} (MeV)
BATSE LAD	60	1.99	28	1.82	100	2.0
BATSE SD	20	1.99	...	...	100	5.8
EGRET TASC	976	300	1061	52.4	1061	52.4
COMPTEL D2	307	10.3	611	10.6	602	10.4
COMPTEL telescope.....	800	30	750	23.4	730	15.0
OSSE	...	...	65	9.5	...	...

To combine spectra from different instruments, the time intervals must either match closely or entirely cover the burst duration. (Light curves for these bursts are presented in many papers, including Fishman et al. 1994 and the above referenced papers.) The time intervals for EGRET, COMPTEL, and OSSE range in duration from 1.024–32.768 s, whereas the BATSE spectral intervals can be as short as 64 ms. Thus, the BATSE time intervals were always chosen to closely match the time intervals from the other instruments. The EGRET and COMPTEL start times are virtually identical and are keyed to the BATSE trigger (Fishman et al. 1994). In general, the time intervals for the final spectra cover the entire burst, so that the start and stop times for individual spectra are not critical. Start and stop times relative to the BATSE trigger time are tabulated in Table 2.

TABLE 2

TIME INTERVALS (IN S) FOR DATA ACCUMULATION WITH RESPECT TO BATSE TRIGGER TIME

Instrument	GRB 910503	GRB 910601	GRB 910814
BATSE	0.00–10.62	0.00–45.37	0.00–33.47
EGRET	0.00–7.00	13.78–46.55	0.00–23.00
COMPTEL.....	0.00–9.00	15.16–33.25	0.00–33.00
OSSE.....	...	1.50–50.65	...

GRB 910503 was the first bright burst seen by BATSE, and it remains one of the brightest BATSE bursts. The burst appeared inside the field of view for the EGRET and COMPTEL instruments. The light curve consists of two distinct and well separated episodes (0–10 and 45–55 s after the BATSE trigger) separated by background. For the energies covered by EGRET and COMPTEL, the first episode had a shorter duration (Schneid et al. 1992; Hanlon et al. 1994). The spectra used cover only the first episode, which contains roughly three-quarters of the burst flux.

GRB 910601 happened to occur in the fields of all four *Compton Gamma Ray Observatory* instruments. The light curve is oddly symmetric, with a total duration of 45 s. The

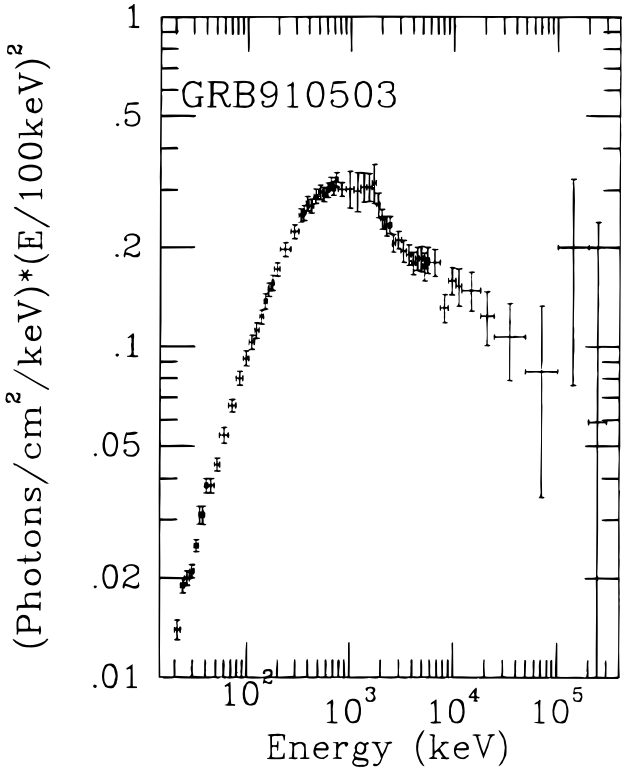

FIG. 1.—Composite spectrum of GRB 910503. The spectrum shows a low-energy portion which is nearly a $\nu^{4/3}$ power law and a peak νF_ν around 1 MeV.

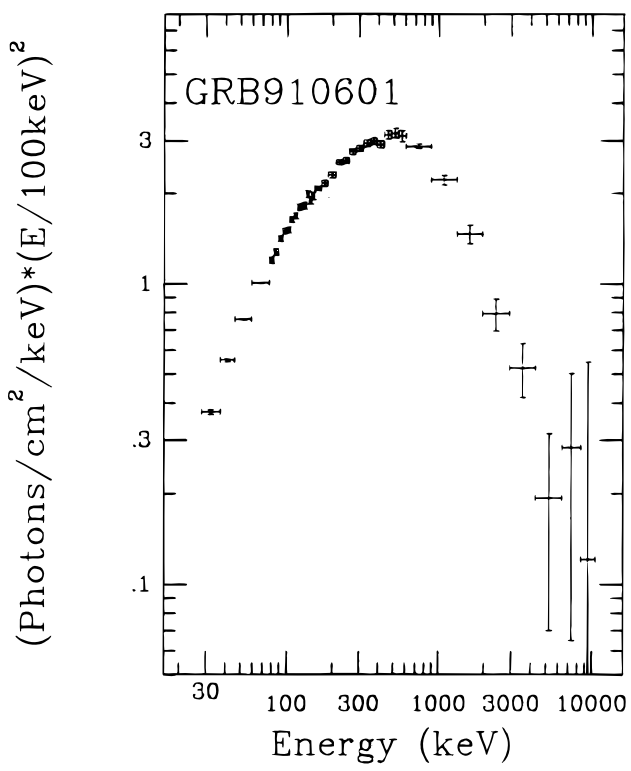

FIG. 2.—Composite spectrum of GRB 910601. The spectrum shows a low-energy portion which is nearly a $\nu^{4/3}$ power law and a peak νF_ν around 500 keV.

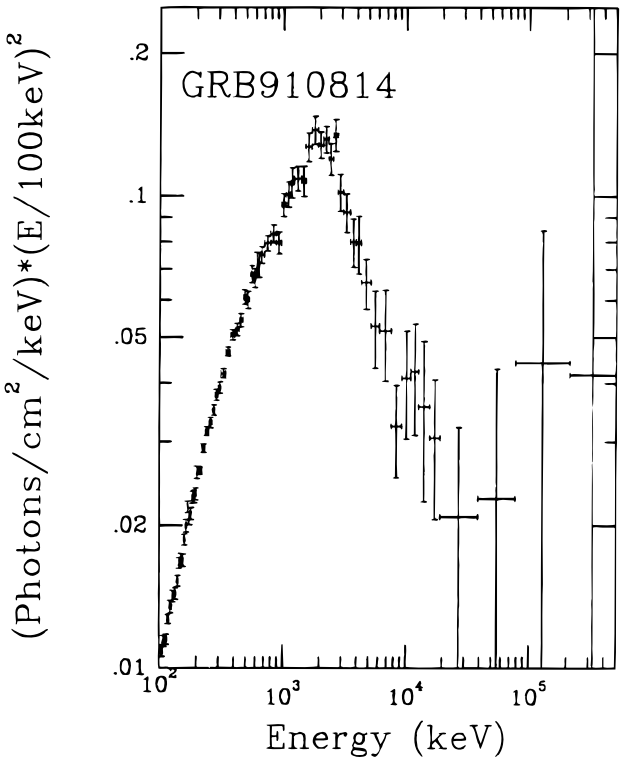

FIG. 3.—Composite spectrum of GRB 910814. The spectrum shows a low-energy portion which is nearly a $\nu^{4/3}$ power law and a remarkably sharp break around 2 MeV.

BATSE trigger was on a relatively small rise roughly 15 s before the time interval with the greatest flux. Roughly 98% of the BATSE flux and 100% of the COMPTEL flux comes in the time interval 15–33 s after the BATSE trigger.

GRB 910814 is a bright burst that appeared in the field of BATSE, COMPTEL, and EGRET. The light curve has a bright initial pulse followed by many overlapping pulses that have smaller amplitude, so that it looks like a ragged exponential decay. The entire COMPTEL flux is contained in the first 33 s time interval (Hanlon et al. 1994), and the BATSE time interval was selected to match this. The entire EGRET flux is contained in the 23 s time interval used (Kwok et al. 1993).

The individual spectra from each instrument are constructed with the observed number of photons divided by the live time for the chosen time interval. Each spectrum is then multiplied by the time interval to form what could be called a "fluence spectrum" which includes all the flux of the burst. Each spectrum is then rebinned in energy to some "standard" template, which is usually the bin boundaries of one of the input spectra. On a bin-by-bin basis, the various instruments are combined as a weighted average. The result is one composite spectrum over a broad energy range for the entire burst fluence.

The spectra are presented as $dN/dE^*(E_{\rm mean}/100\ {\rm keV})^2$ which is proportional to νF_ν. $E_{\rm mean}$ is the geometric mean of the bin boundaries. This value flattens out the steeply falling curve to allow for easier visibility of deviations from a power law. Spectra presented as νF_ν also have the advantages of displaying the energy in a frequency interval as well as being the form used for comparison with theoretical models (e.g., Katz 1995; Tavani 1996). The spectra are then rebinned as appropriate to an energy resolution approximating that of the instruments. The final results are presented in Table 3–5 and Figures 1–3.

These spectra are presented quantitatively so that theorists can test emission mechanism models over a wide energy range. For example, they can test magnetic photon

TABLE 3

SPECTRUM OF GRB 910503

$E_{\rm low}$ (keV)	νF_ν
20	0.014 ± 0.001
23	0.019 ± 0.001
25	0.020 ± 0.001
28	0.021 ± 0.001
31	0.025 ± 0.001
34	0.031 ± 0.002
36	0.031 ± 0.002
39	0.038 ± 0.002
42	0.038 ± 0.002
48	0.044 ± 0.002
54	0.054 ± 0.003
66	0.066 ± 0.003
78	0.080 ± 0.004
91	0.092 ± 0.005
104.....	0.103 ± 0.005
117.....	0.112 ± 0.006
130.....	0.123 ± 0.006
143.....	0.137 ± 0.007
156.....	0.149 ± 0.007
169.....	0.156 ± 0.008
182.....	0.171 ± 0.008
209.....	0.197 ± 0.010
263.....	0.224 ± 0.011
317.....	0.251 ± 0.012
344.....	0.255 ± 0.013
371.....	0.273 ± 0.014
399.....	0.268 ± 0.013
444.....	0.288 ± 0.014
489.....	0.295 ± 0.015
535.....	0.291 ± 0.015
580.....	0.300 ± 0.015
625.....	0.313 ± 0.015
669.....	0.304 ± 0.015
712.....	0.323 ± 0.016
756.....	0.301 ± 0.015
906.....	0.303 ± 0.039
1081	0.298 ± 0.041
1257	0.306 ± 0.031
1432	0.306 ± 0.030
1608	0.315 ± 0.043
1784	0.270 ± 0.024
1945	0.245 ± 0.017
2138	0.234 ± 0.017
2332	0.235 ± 0.014
2526	0.206 ± 0.013
2721	0.211 ± 0.013
3108	0.195 ± 0.015
3496	0.190 ± 0.014
3883	0.179 ± 0.014
4271	0.185 ± 0.015
4659	0.185 ± 0.017
5046	0.175 ± 0.017
5434	0.183 ± 0.017
5825	0.180 ± 0.017
7375	0.131 ± 0.013
8926	0.158 ± 0.015
10476	0.152 ± 0.020
12021	0.148 ± 0.020
18221	0.124 ± 0.023
24422	0.107 ± 0.028
49244	0.084 ± 0.049
100380.....	0.200 ± 0.124
199580.....	0.059 ± 0.180
300000.....	

TABLE 4

SPECTRUM OF GRB 910601

E_{low} (keV)	νF_ν
28.....	0.374 ± 0.007
37.....	0.556 ± 0.007
46.....	0.760 ± 0.005
59.....	1.008 ± 0.005
77.....	1.200 ± 0.029
82.....	1.277 ± 0.030
88.....	1.415 ± 0.032
94.....	1.495 ± 0.034
100	1.512 ± 0.036
105	1.632 ± 0.038
111	1.688 ± 0.041
117	1.799 ± 0.044
123	1.811 ± 0.046
128	1.818 ± 0.049
134	1.989 ± 0.053
140	1.899 ± 0.055
146	1.964 ± 0.059
152	2.081 ± 0.039
169	2.166 ± 0.047
186	2.305 ± 0.050
209	2.537 ± 0.052
233	2.577 ± 0.061
256	2.758 ± 0.060
285	2.827 ± 0.063
320	2.942 ± 0.072
355	2.998 ± 0.080
391	2.911 ± 0.088
438	3.150 ± 0.105
486	3.181 ± 0.119
541	3.112 ± 0.133
601	2.871 ± 0.051
888	2.219 ± 0.083
1318	1.462 ± 0.102
1949	0.792 ± 0.097
2910	0.523 ± 0.107
4310	0.193 ± 0.123
6387	0.284 ± 0.219
8464	0.121 ± 0.426
10541.....	

splitting and pair production models (Baring 1990, 1993) and the synchrotron shock model (Tavani 1996).

3. COMPOSITE OF BRIGHT BATSE SPECTRA

We have constructed composite spectra by combining many spectra from bright GRBs. Such a composite can be used to search for faint spectral lines present in many bursts. The composite can also be used as an "average" spectral shape, for example, to calculate redshift corrections in cosmological models.

Our composite was constructed for bright bursts as given in the BATSE spectroscopy detector catalog (Schaefer et al. 1994). Various subsets of bursts were used: the 20 events with data above 50 keV, the 19 events with data above 40 keV, the six events with data above 30 keV, the seven brightest events with data above 50 keV, and the 13 faintest events with data above 40 keV. All subsets return closely similar spectra with the shape being identical to within error bars. In particular, the faint events have a similar combined spectrum as the bright events, showing that the composite is not dominated by a few bright events. The spectrum from 30 to 40 keV is a simple power-law extension of the slope above 40 keV.

The composite was constructed from individual deconvolved spectra which cover the entire burst data. The first

TABLE 5

SPECTRUM OF GRB 910814

E_{low} (keV)	νF_ν
103.....	0.0109 ± 0.0003
108.....	0.0114 ± 0.0003
112.....	0.0115 ± 0.0003
117.....	0.0127 ± 0.0003
122.....	0.0135 ± 0.0004
127.....	0.0142 ± 0.0004
132.....	0.0144 ± 0.0004
138.....	0.0153 ± 0.0004
143.....	0.0167 ± 0.0004
148.....	0.0170 ± 0.0005
153.....	0.0169 ± 0.0005
158.....	0.0187 ± 0.0005
163.....	0.0200 ± 0.0006
168.....	0.0219 ± 0.0006
173.....	0.0207 ± 0.0006
178.....	0.0212 ± 0.0006
183.....	0.0229 ± 0.0007
189.....	0.0230 ± 0.0007
194.....	0.0233 ± 0.0007
199.....	0.0259 ± 0.0008
204.....	0.0261 ± 0.0005
220.....	0.0291 ± 0.0006
235.....	0.0316 ± 0.0007
251.....	0.0330 ± 0.0008
267.....	0.0351 ± 0.0009
282.....	0.0378 ± 0.0010
298.....	0.0391 ± 0.0011
314.....	0.0419 ± 0.0010
341.....	0.0466 ± 0.0011
373.....	0.0506 ± 0.0013
405.....	0.0520 ± 0.0016
437.....	0.0544 ± 0.0018
469.....	0.0610 ± 0.0022
502.....	0.0601 ± 0.0026
534.....	0.0682 ± 0.0029
567.....	0.0670 ± 0.0031
600.....	0.0719 ± 0.0041
621.....	0.0716 ± 0.0044
643.....	0.0750 ± 0.0031
698.....	0.0795 ± 0.0030
786.....	0.0831 ± 0.0036
874.....	0.0796 ± 0.0042
962.....	0.0957 ± 0.0053
1051	0.1008 ± 0.0064
1140	0.1067 ± 0.0078
1229	0.1088 ± 0.0066
1407	0.1076 ± 0.0079
1520	0.1270 ± 0.0089
1702	0.1379 ± 0.0094
1916	0.1281 ± 0.0082
2129	0.1317 ± 0.0086
2343	0.1198 ± 0.0094
2557	0.1346 ± 0.0105
2770	0.1019 ± 0.0092
3091	0.0923 ± 0.0087
3518	0.0799 ± 0.0094
3945	0.0795 ± 0.0111
4372	0.0654 ± 0.0080
5227	0.0528 ± 0.0099
6081	0.0516 ± 0.0114
7576	0.0324 ± 0.0072
9285	0.0410 ± 0.0106
10994	0.0423 ± 0.0112
12703	0.0357 ± 0.0133
15693	0.0306 ± 0.0100
19111	0.0209 ± 0.0114
38762	0.0228 ± 0.0200
78065	0.0442 ± 0.0404
211351.....	0.0416 ± 0.3255
500000.....	

step was to rebin each input spectrum into a template of "standard" bin boundaries. The second step was to combine all spectra (on a bin-by-bin basis) with a weighted average. The third step was to combine bins in the averaged spectrum to just under the energy resolution of the BATSE spectroscopy detectors. The fourth step was to multiply the dN/dE values by $(E_{\rm mean}/100\ {\rm keV})^2$ to get vF_v values.

Figure 4 and Table 6 present the composite spectrum for 19 bright BATSE bursts from 41 to 1932 keV. The average vF_v slope is close to flat, certainly in comparison to the three bursts described in § 2.

TABLE 6

COMPOSITE SPECTRUM OF BRIGHT BATSE BURSTS

$E_{\rm low}$ (keV)	vF_v
41	0.0053 ± 0.0003
43	0.0052 ± 0.0003
45	0.0049 ± 0.0003
47	0.0050 ± 0.0003
49	0.0049 ± 0.0003
50	0.0054 ± 0.0003
52	0.0057 ± 0.0003
54	0.0057 ± 0.0002
58	0.0061 ± 0.0002
62	0.0065 ± 0.0002
66	0.0071 ± 0.0002
70	0.0073 ± 0.0003
74	0.0073 ± 0.0003
78	0.0071 ± 0.0003
82	0.0083 ± 0.0003
86	0.0084 ± 0.0003
90	0.0086 ± 0.0003
94	0.0090 ± 0.0003
98	0.0098 ± 0.0003
103.....	0.0092 ± 0.0003
107.....	0.0091 ± 0.0003
111.....	0.0100 ± 0.0004
115.....	0.0103 ± 0.0004
119.....	0.0095 ± 0.0004
123.....	0.0098 ± 0.0004
127.....	0.0106 ± 0.0004
131.....	0.0110 ± 0.0004
135.....	0.0106 ± 0.0005
139.....	0.0110 ± 0.0005
144.....	0.0104 ± 0.0005
148.....	0.0108 ± 0.0005
152.....	0.0110 ± 0.0005
156.....	0.0106 ± 0.0005
160.....	0.0122 ± 0.0006
164.....	0.0108 ± 0.0006
169.....	0.0107 ± 0.0006
173.....	0.0111 ± 0.0006
177.....	0.0120 ± 0.0007
181.....	0.0106 ± 0.0007
185.....	0.0126 ± 0.0004
202.....	0.0124 ± 0.0004
219.....	0.0115 ± 0.0004
236.....	0.0123 ± 0.0005
253.....	0.0122 ± 0.0005
270.....	0.0115 ± 0.0006
288.....	0.0119 ± 0.0007
305.....	0.0116 ± 0.0007
322.....	0.0134 ± 0.0008
339.....	0.0118 ± 0.0008
357.....	0.0116 ± 0.0009
374.....	0.0132 ± 0.0010
391.....	0.0118 ± 0.0011
408.....	0.0135 ± 0.0011
425.....	0.0117 ± 0.0012
443.....	0.0102 ± 0.0013
460.....	0.0109 ± 0.0014
477.....	0.0119 ± 0.0016
494.....	0.0109 ± 0.0019
512.....	0.0125 ± 0.0015
546.....	0.0123 ± 0.0014
581.....	0.0082 ± 0.0015
614.....	0.0122 ± 0.0017
648.....	0.0122 ± 0.0019
681.....	0.0093 ± 0.0021
715.....	0.0096 ± 0.0014
798.....	0.0067 ± 0.0014
932.....	0.0062 ± 0.0018
1065.....	0.0067 ± 0.0023
1198.....	0.0172 ± 0.0030
1332.....	0.0045 ± 0.0037
1465.....	0.0018 ± 0.0043
1599.....	0.0067 ± 0.0051
1732.....	0.0067 ± 0.0057
1865.....	0.0158 ± 0.0130
1899.....	0.0093 ± 0.0130
1932.....	

The bursts for each composite spectrum are averaged together so that a high fluence burst will receive a higher weight than a low fluence burst. The 19 burst composite has events with fluences (50–300 keV; Fishman et al. 1994) ranging from 1.4×10^{-6} to 5.3×10^{-5} ergs cm^{-2} with a median of 4.4×10^{-6} ergs cm^{-2}. Half of the total fluence comes from the four brightest bursts. The 13 burst composite has events with fluences ranging from 1.4×10^{-6} to 8.5×10^{-6} ergs cm^{-2}, with a median of 3.9×10^{-6} ergs cm^{-2}. Half of the total fluence comes from the five brightest bursts.

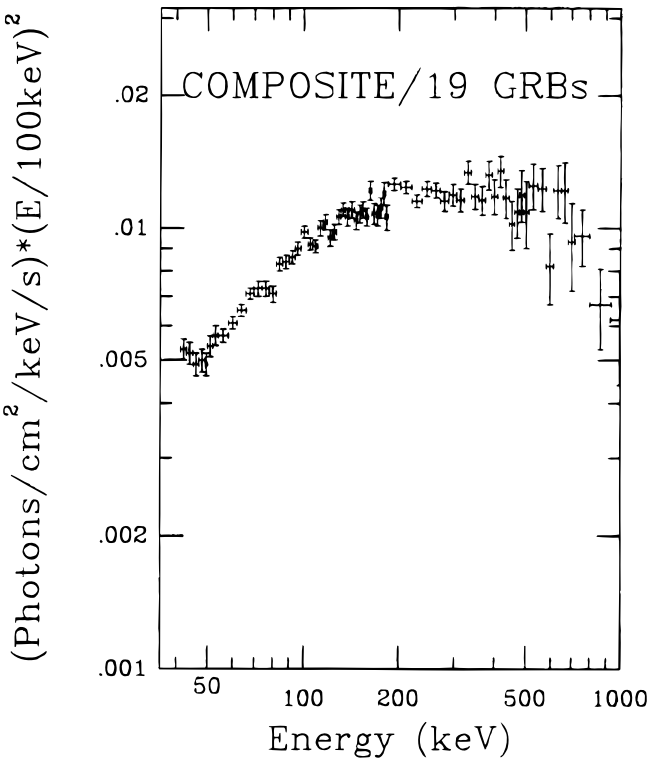

FIG. 4.—Composite spectrum of 19 bright BATSE bursts. The spectrum is relatively flat as it is composed of some bursts with flat spectra and others with peaks over a wide range of energy.

The peak flux can be used as a distance indicator. For the 19 burst composite, the median peak flux in a 256 ms time bin is 6.5 photons s^{-1} cm^{-2} (Fishman et al. 1994). For typical cosmological models (e.g., Wickramasinghe et al. 1993; Malozzi et al. 1995; Fenimore et al. 1993), this corresponds to $z \sim 0.4$. For the 13 burst composite, the median peak flux is 4.2 photons s^{-1} cm^{-2}, which corresponds to $z \sim 0.5$.

It is possible that some weak narrow line that appears in many burst spectra (at the same energy) could be significant in the composite spectra. This would not be the case for lines from GRBs with differing redshifts or relativistic boost factors. Unfortunately, no significant spectral lines appear either in Figure 4 or in any other composite spectrum we have created. The quantitative limits have complex dependencies on the energy, the confidence threshold, and the line width for each composite spectrum (Ford et al. 1993; Palmer et al. 1993). However, to give two specific limits of interest, a narrow line at 500 keV must have equivalent widths of less than 11 and 24 keV at the 99% confidence level for the 19 burst and 13 burst composite spectra, respectively.

The spectral shape is straighter and flatter than for the individual bursts from § 2. We believe that this apparent difference arises from two causes. First, the composite extends over a narrower energy range (41–1932 keV) than the three individual bursts, so that any curvature will be less apparent. Second, the composite is an average over many spectral shapes with a wide range of peak energies. A perusal of the input spectra shows some that are closely flat (e.g., GRB 910930 and GRB 911127), some that are nearly flat (e.g., GRB 910630 and GRB 911104), and others that peak over a wide range of energies (from 150 keV for GRB 910927 to 500 keV for GRB 910630 to 1300 keV for GRB 910814). The result of combining these various spectral shapes will be relatively flat composite spectrum.

4. LOW-ENERGY SLOPE

Many models of GRBs envision an expanding fireball since there are no plausible mechanisms to contain an explosion of the required energy. The properties of this fireball are expected to be independent of the detailed scenario leading to the energy release and, indeed, are applicable for either galactic halo or extragalactic distances. The fireball will interact with a surrounding low-density gas to form a relativistic collisionless shock that radiates primarily by optically thin synchrotron (Mészáros & Rees 1993; Katz 1994; Tavani 1996). Katz (1994) has presented general arguments that the spectral shape for GRBs will asymptote to $\nu F_\nu \propto \nu^{4/3}$ at low energies. Thus, many burst spectra should fit well to a $\nu^{4/3}$ power law at energies below some turnover energy. The position of the turnover depends on details of the electron distribution, but the logarithmic spectral slope at low energies should never be greater than 4/3. The superposition of multiple spectra with this property will also satisfy the same property.

This prediction can be tested with the spectra in this paper. For GRB 910503, the νF_ν spectrum from 20 to 100 keV is best fit by a power law of index 1.20. For GRB 910601, the νF_ν spectrum from 28 to 100 keV is best fit by a power law of index 1.22. For GRB 910814, the νF_ν spectrum from 103 to 200 keV is best fit by a power law of index 1.32. The composite spectrum has a νF_ν spectrum from 41 to 100 keV with a best-fit power law of index 0.77. These results are in agreement that $\alpha \leq 1.33$ for νF_ν scaling as ν^α. More exciting is the close match between the predicted index below the turn over ($\alpha \approx 1.33$) and the observed value for these spectra.

The prediction can also be tested with various data sets from the BATSE and *Ginga* instruments. Four papers present spectral fits from which a low-energy spectral slope can be deduced (Schaefer et al. 1994; Preece et al. 1996; Band et al. 1993; Strohmayer et al. 1997). Two types of models have been fitted, one a sharply broken power law (SBPL) and the other a smoothly broken power law (the "GRB" model of Band et al. 1993). In both cases, the required spectral continuity across the break may create biases depending on the intrinsic spectral shape. With an SBPL, a spectrum that curves smoothly will yield a low-energy spectral slope that is biased toward lower values. This effect is minimal if the curvature is either sharp or small. A choice of a restricted energy range over which the curvature is minimal should yield a reliable low-energy spectral slope. With the GRB model, a spectrum with sharp curvature will yield a low-energy spectral slope that is biased toward higher values. In addition, the GRB model connects the high- and low-energy slopes through the break energy so that a spectrum with a low break energy can have the high energy dominate the fit and force unrealistic low-energy spectral slopes.

Schaefer et al. (1994) report spectral fits for bright BATSE bursts with the spectroscopy detector. The low-energy behavior is represented for SBPL fits for energies less than 500 keV (see Table 7 of Schaefer et al. 1994). Over this energy range, the spectral curvature is minimal (see figures in Schaefer et al. 1994), so these fits should yield a reliable measure of the low-energy spectral slope. The tabulated low-energy spectral index must be raised by 2.0 to yield the νF_ν index. All 24 bright burst spectra obey the prediction that $\alpha \leq 1.33$. The highest α value is 1.25 and the median α value is 0.70, in good agreement with the prediction that the indices for many bursts will appoach the limit of 1.33.

Band et al. (1993) report spectral fits for 54 bright BATSE bursts with the spectroscopy detector, with substantial overlap with the spectra in Schaefer et al. (1994). For each burst, a fit to the GRB model is reported with parameters α and E_0. The spectral slope at the lowest observed energy (E_1 from their Table 1) will be $\alpha - E_1/E_0$. Of the 54 bursts, 12 have slopes that significantly violate Katz's prediction. Of these 12, there are a variety of concerns: first, scattered photons from the spacecraft and earth were not corrected for. These will add flux which peaks sharply around 50 keV (Hua & Lingenfelter 1993) so as to create an artificially high spectral slope at low energies. The scattered component from Earth is important for several of the 12 bursts (e.g., GRB 10709 and GRB 920513−60781), while all data will have scattered light from the spacecraft. Second, the reported high spectral slope for many of the 12 bursts is greatly inconsistent with the photon spectra presented elsewhere. For example, GRB 910507 and GRB 911016 have reported low-energy spectral slopes greatly different than appear in Figures 12 and 28 of Schaefer et al. (1994). In particular, when the GRB model with a low E_0 value is used a fitted low-energy slope can be substantially different from that obtained by a simpler model whose slope agrees with Katz's prediction. Third, the remaining spectra have individual problems. For example, GRB 911217 is during a solar flare so the determination of the background can

never be made reliably, especially at low energies, and GRB 911106 has a long data gap starting during the burst which results in no reliable background data. In summary, not one of the 12 bursts which apparently violate Katz's limit can be considered to have a reliable low-energy spectral slope.

Preece et al. (1996) reports fits to the GRB model for 86 bright bursts with the BATSE spectroscopy detectors. They have made a significant advance in using the lowest discriminator channel which provides a single point with a typical energy range of 6–10 keV. They report that 12 bursts have significant excess in the discriminator channel relative to the GRB model. From their Figure 6, there are 11 bursts which apparently violate Katz's prediction, based on fits with smoothly broken power-law models. Preece (1997, private communication) reports that these violators are not the bursts with low-energy excesses and that the error bars are sufficiently small to excuse the violations. However, Preece notes that if a SBPL is chosen as the continuum model, then the low-energy spectral slopes no longer violate the Katz limit. In this situation of imperfect knowledge, we conclude that certainly the majority ($>87\%$) of bursts obey Katz's prediction, while the remainder might also obey.

Strohmayer et al. (1997) presents spectra and fits for 16 bursts with *Ginga* data from 2–400 keV. A substantial problem for all but two bursts is that the position on the sky is unknown, so that the detector response can only be calculated for some assumed angle. Their Figure 1 shows that the effect of an incorrect angle is to drastically change the deduced slope at energies below ~ 5 keV. With this, 15 of the 16 *Ginga* spectra are seen to fit Katz's prediction for the low-energy slope. The one exception is GRB 870303, for which a cyclotron line has been reported (Murakami et al. 1988). This is one of the bursts for which a position is known, so the detector response is reliably known. This burst has a spectral slope in accordance with Katz's prediction above an energy of ~ 5 keV, yet has a significant violation ($\nu F_\nu \propto \nu^2$) from 2 to 5 keV. As such, this spectrum does appear to violate Katz's model.

In summary, the Katz prediction for the asymptotic low-energy spectral slope ($\nu F_\nu \propto \nu^{4/3}$) easily fits the majority (greater than $\sim 90\%$) of all bursts. There are a few possible cases that might violate Katz's prediction, however the evidence for these violations is weak due to unresolved serious problems. Only one spectrum (GRB 870303 with *Ginga*) apparently disobeys the prediction for which there are no known problems.

REFERENCES

Band, D. L., et al. 1993, ApJ, 413, 281
Baring, M. G. 1990, MNRAS, 244, 49
———. 1993, ApJ, 418, 391
Fenimore, E. E., et al. 1993, Nature, 366, 40
Fishman, G. J., et al. 1994, ApJS, 92, 229
Ford, L. A., et al. 1993, in AIP Conf. Proc. 280, Compton Gamma-Ray Observatory, ed. M. Friedlander, N. Gehrels, & D. J. Macomb (New York: AIP), 887
Hanlon, L. O., et al. 1994, A&A, 285, 161
Hua, X.-M., & Lingenfelter, R. E. 1993, in Compton Gamma-Ray Observatory, ed. M. Friedlander, N. Gehrels, & D. J. Macomb (New York: AIP), 927
Katz, J. I. 1994, ApJ, 432, L107
Kwok, P. W., et al. 1993, in AIP Conf. Proc. 280, Compton Gamma-Ray Observatory, ed. M. Friedlander, N. Gehrels, & D. J. Macomb (New York: AIP), 855
Mallozzi, R. S., et al. 1995, ApJ, 454, 597
Mészáros, P., & Rees, M. J. 1993, ApJ, 405, 278
Murakami, T., et al. 1988, Nature, 335, 234
Palmer, D. M., et al. 1993, in AIP Conf. Proc. 280, Compton Gamma-Ray Observatory, ed. M. Friedlander, N. Gehrels, & D. J. Macomb (New York: AIP), 892
Preece, R. D., et al. 1996, ApJ, 473, 310
Schaefer, B. E., et al. 1994, ApJS, 92, 285
Schneid, E. J., et al. 1992, A&A, 255, L13
Share, G. H., et al. 1992, in AIP Conf. Proc. 265, Gamma-Ray Bursts, ed. W. S. Paciesas & G. J. Fishman (New York: AIP), 32
———. 1994, in AIP Conf. Proc. 307, Gamma-Ray Bursts, ed. G. J. Fishman, J. J. Brainerd, & K. Hurley (New York: AIP), 283
Strohmayer, T. E., Fenimore, E. E., Murakami, T., & Yoshida, A. 1997, ApJ, submitted
Tavani, M. 1996, Phys. Rev. Lett., 76, 3478
Wickramasinghe, W. A. D. T., et al. 1993, ApJ, 411, L55
Winkler, C., et al. 1992, A&A, 255, L9
———. 1993, in AIP Conf. Proc. 280, Compton Gamma-Ray Observatory, ed. M. Friedlander, N. Gehrels, & D. J. Macomb (New York: AIP), 845